



Experimental and analytical study of the influence of the incident heat flux in cables heat release

David Lázaro¹ · Alain Alonso¹ · Mariano Lázaro¹ · Miguel Ángel Jiménez² · Daniel Alvear³

Received: 1 November 2022 / Accepted: 14 March 2023 / Published online: 6 April 2023
© The Author(s) 2023

Abstract

Cone calorimeter is widely used to study fire behaviour of materials employing small size samples. This equipment allows obtaining parameters such as time to ignition (TTI), heat of combustion, mass loss rate (MLR), or heat release rate (HRR) under different heat fluxes. Some studies have considered a linear fitting between MLR and HRR peaks and the incident heat flux. In accordance with this hypothesis, the computer model Fire Dynamics Simulator (FDS) has included a simple model to extrapolate burning rate data collected from a cone calorimeter test to the heat feedback occurring during a simulation. Nevertheless, deviation in the prediction of the HRR peaks at 75 kW m^{-2} of approximately 39.3% and of 37.1% for the first and second peak, respectively, were found. Therefore, this work presents a correlation between the incident heat flux and the global HRR per unit area curve, testing up to five different cables and several heat fluxes. To do so, some modifications of the FDS correlation are performed to consider the effect of the flame heat flux in the decomposition of the cables. Once experimental data are acquired, a computational analysis is carried out using FDS to achieve the flame heat flux in the samples. Additionally, this flame heat flux has also been obtained from the literature. As a conclusion, the addition of the flame heat flux to the cone calorimeter incident heat flux provides better predictions than the linear fitting methodology defined in the FDS Guide. Furthermore, this correction is checked with: (1) the example included in FDS guide, decreasing the HRR peaks errors from around 38% to around 25%; and (2) to seven different cables from the literature, decreasing the HRR peaks relative errors, as average, from 14.2 to 9.5% approximately.

Keywords Cone calorimeter · Cable · Polymers · HRR

Introduction

In the past, cable tray installations have fueled fires that resulted in serious damage to nuclear power plants (NPP). Among others, it can be highlighted some incidents like: (1) Browns Ferry NPP incident, caused by a fire in the cable spreading room [1]; (2) fire in Armenia NPP, where the fire was initiated by a short in the power circuits inside cable galleries, and propagated rapidly until it became a large fire [2]; and (3) in Beloyarsk NPP where the fire started in the turbine building due to a break in the oil system, and it

propagated to cables and from there into the control building [2].

Nevertheless, the study and prediction of cable fire propagation is a very complex issue. In fact, cable fire modelling is a key priority to be solved as it is noted in the research activities FY 2018–2020 defined by the U. S. Nuclear Regulatory Commission in the last revision of the NUREG 1925 [3]. Furthermore, four of the research programs described in the NUREG 1925 are directly related with the understanding and prediction of cable fire propagation. One of these programs is the Cable Heat Release, Ignition, and Spread in Tray Installations during Fire (CHRISTIFIRE) [4, 5]. This program includes fire tests on grouped electrical cables to enable better understanding of the fire hazard characteristics including the ignition, heat release rate, and flame spread. The U.S. Nuclear Regulatory Commission (NRC) used this type of quantitative information to develop a simple model of upward fire spread in horizontal tray configurations, called FLASH-CAT (Flame Spread over Horizontal

✉ David Lázaro
lazarod@unican.es

¹ Universidad de Cantabria, Santander, Spain

² Consejo de Seguridad Nuclear, CSN, Madrid, Spain

³ General Directorate of Industry, Energy and Mines,
Government of Cantabria, Santander, Spain

Cable Trays) model. Nevertheless, FLASH-CAT model makes some important assumptions: (1) the cable trays are horizontal and stacked vertically with a spacing of less than 0.45 m; (2) the cables burn in the open air; (3) the cables are only exposed to the ignition source below them; (4) it only considers the cables as either thermoplastic or thermoset; (5) the effect of the heat released by the ignition source at the ignition time of the lower cable tray is not taken into account. To analyse the fire propagation along different cable trays configurations, and to consider the effect of the oxygen availability in the combustion, it is required the use of more complex fire models.

Fire Dynamics Simulator (FDS) [6] is a computational fire model that allows analysing low-speed flows during a fire, with an emphasis on smoke and heat transport from fires. Nevertheless, the complexity of modelling cable fire propagation is a challenge which makes it currently not validated in FDS validation guide [7]. One of the goals of the PRISME 3 project by the OECD/NEA—Fire Propagation in Elementary, Multi-Room Scenarios program (described in the NUREG 1925 [3])—is to provide experimental data that allows defining, calibrating and validating the fire models to predict cable fire propagation. In the framework of the PRISME 3 programme, a benchmark exercise on a realistic cable fire scenario in an electrical system was carried out. The results showed that even using complex models like FDS, fire propagation prediction is highly affected by the model definition and input parameters selected for the definition of the cables [8].

The simplest approach could be imposing the HRR per unit area and the horizontal propagation rate [9] obtained experimentally. Another common approach is to consider an ignition temperature and a HRR per unit area upon reaching this temperature [10], or by means of the burning rate [11]. And, for example, to model the scenario CFSS1 from PRISME [12], in [13], the cables are defined using the ignition temperature and the HRR per unit area obtained from the cone calorimeter experimental tests. Nevertheless, in all previous works, the imposed HRR per unit area in the cables is fixed independently of the incident heat fluxes that are really affecting the cables during the simulations. However, the influence of the incident heat flux on the HRR per unit area is well-known and widely documented in the literature [14], and it affects the heat release by the cable, and hence, the fire propagation.

In order to improve the way to represent the fire behavior of cables, FDS [6] has included a simple model to extrapolate burning rate data (e.g. MLR or HRR per unit area) collected from a cone calorimeter or a similar device to the

heat feedback occurring during an FDS simulation. To do so, the heat flux at which the cone calorimeter test was executed can be defined. When a wall cell reaches the ignition temperature, this model starts marching along the test data curve using a scaled timestep where the scaled timestep is the FDS timestep adjusted by the ratio of cone heat flux to the FDS incident flux. At the scaled time, the ramp output is scaled by the ratio of the FDS incident flux to the cone heat flux. Similar linear fitting between the incident heat flux and the MLR and HRR peaks was studied in [15] for a flame-retardant ethylene-propylene-diene monomer rubber. The results showed a linear fitting between MLR and HRR peaks and the heat flux. Nevertheless, in the demonstration of extrapolating cone test data to other incident heat fluxes included in [6], it is observed a deviation in the prediction of the HRR peaks at 75 kW m^{-2} of approximately 39.3% and of 37.1% for the first and the second peaks, respectively. Having said that, the actual incident heat flux at which samples are decomposed includes the external heat flux (cone calorimeter heat flux) and the flame heat flux, and it is not considering in FDS Guide.

In the present work, it is included a correlation analysis between incident heat flux and the global HRR curve, testing up to five different cables and considering several heat fluxes. The study analyses the direct linear fitting defined in [6] that considers the cone calorimeter incident heat flux. Furthermore, it presents two different methodologies to consider the effect of the flame heat flux in the cone calorimeter results. Considering the flame heat flux, an improvement of the results of the correlation between cone calorimeter HRR curves for different incident heat fluxes can be observed.

Materials and method

This work employed up to five cable types to analyse the applicability of the method. Table 1 defines the different cables including the name, class (according to Euroclasses), external diameter and sheath and insulation materials. The Eca class undertakes a basic vertical flame test to BS EN 60332-1-2 [16]. Cables with an Eca class are combustible with a limited fire spread, and is the minimum cable requirement for general installations. The classes Cca and B2ca are obtained by performing the reaction to fire tests EN 50399 [17]. Cables with a Cca class are combustible with a moderate flame spread and heat release. These cables are commonly used in public buildings, hotels, schools, or office buildings. Finally, cables with a B2ca class are also combustible with low flame spread and low heat release

Table 1 Selected cables and properties

Cable	Class	Cable diam./mm	Sheath mass/kg m ⁻¹	Insulation mass/kg m ⁻¹	Metal mass/kg m ⁻¹	Sheath material	Insulation material
RV-k 0.6/1 kV 3×1.5 mm ²	Eca	9.1	0.068	0.014	0.035	Polyvinyl chloride PVC	Cross-linked polyethylene XLPE
RV-k 0.6/1 kV 3×4 mm ²	Eca	10.7	0.082	0.020	0.093	Polyvinyl chloride PVC	Cross-linked polyethylene XLPE
RZ1-K AS 3×1.5 mm ²	Cca	9.67	0.082	0.015	0.035	Halogen-free thermoplastic polyolefin	Cross-linked polyethylene XLPE
RZ1-K AS 5×1.5 mm ²	Cca	12.24	0.134	0.028	0.058	Halogen-free thermoplastic polyolefin	Cross-linked polyethylene XLPE
H07Z1-K 1×50 mm ²	B2ca	12.15	0.067	-	0.354	Halogen-free thermoplastic polyolefin	-

contribution to fire. Actually, B2ca is the highest class for commercial cables.

The sections of the cables are represented in Fig. 1. As we can see, the cables RV-k 0.6/1 kV 3×1.5 mm² and RV-k 0.6/1 kV 3×4 mm² are of the same family, but with different core section, external diameter and the thickness of sheath and insulation materials. These cables use PVC as sheath and XLPE as insulation. The cables RZ1-K AS 3×1.5 mm² and RZ1-K AS 5×1.5 mm² belongs to the same family but have different number of cores, external diameters and material distribution. Finally, the cable H07Z1-K 1×50 mm² only has the sheath of Halogen-free thermoplastic polyolefin. This is the unique cable studied in the present work that does not have XLPE. As shown in the thermal analysis collected in [18, 19], the PE is much more energetic than the PVC.

The method employed in the present work to define and validate the proposed methodologies to extrapolate

the cone calorimeter HRR per unit area between different incident heat fluxes is divided in the following stages:

- Cone calorimeter test for the cables
- Validation of the original methodology
- Modifications of the methodology
- Validation of the modifications.

The proper definition of the experimental tests, considering relevant boundary conditions definition and ensuring repeatability, is crucial to assess a valid correlation. While defining the cone calorimeter test, it is important to define an appropriate incident heat flux. A value too small can delay the ignition, or even makes ignition to not take place. On the other hand, a value too large can accelerate decomposition of the sample reducing the information about reactions. Most typical values for the cone calorimeter heat flux are 25 kW m⁻², 50 kW m⁻² and 75 kW m⁻². In the present work, we have performed test under 50 kW m⁻² and 75 kW m⁻²

Fig. 1 Cables used in the study: **a** RV-k 0.6/1 kV 3×1.5 mm²; **b** RV-k 0.6/1 kV 3×4 mm²; **c** RZ1-K AS 3×1.5 mm²; **d** RZ1-K AS 5×1.5 mm²; **e** H07Z1-K 1×50 mm²

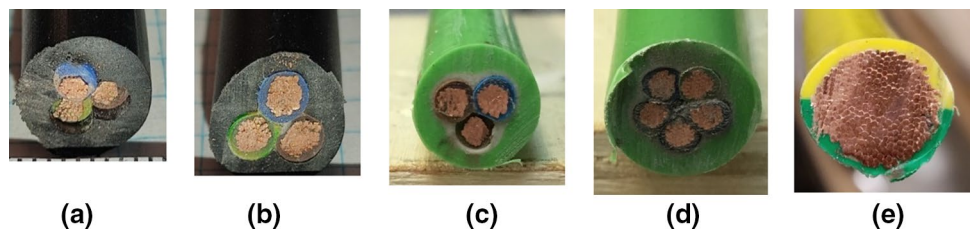
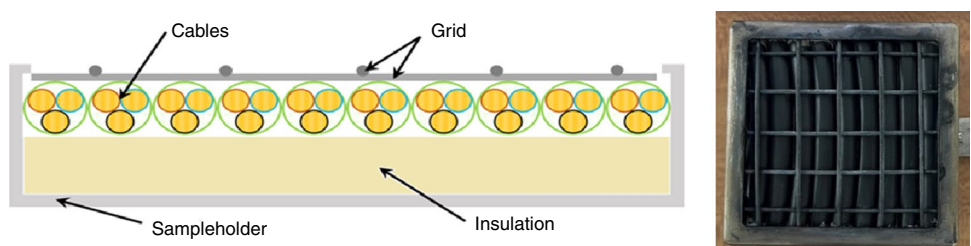


Fig. 2 Disposition of the cables in the cone calorimeter sample holder



for all cases, and also at 25 kW m^{-2} for two cables. The disposition of the cables in the sample holder is also very important, and it follows the description performed in the ISO 5660 [20] and in [14]. Figure 2 shows the disposition of the cables in the sample holder, with the grid and insulation location. Repeatability tests have been performed for each experiment including in the result section the average of the experimental HRR per unit area curves.

Once the test campaign was finished, the validation of the linear fitting proposed in the FDS Guide is performed in the second stage of the method. To do this, the experimental cone calorimeter tests under the heat flux of 50 kW m^{-2} are considered as the base ones, that will be used for the extrapolation to the other heat fluxes (75 kW m^{-2} and 25 kW m^{-2}). This heat flux is considered as a reference because it is the most employed one, and is very common to find it in the literature. Experimental HRR per unit area curves obtained for the different cables are compared with the predicted ones.

Then, in the third stage, a model of the cone calorimeter test under the heat fluxes of 50 and 75 kW m^{-2} was developed in FDS for the different cables. The temperatures of the cone calorimeter resistance model are calibrated to assess the desired heat fluxes on the exposed surface of an inert sample. After that, the experimental HRR per unit area curves are imposed in the samples of the model. After the simulations are run, the flame heat flux can be calculated as the difference between the simulated total incident heat flux on the sample and the imposed by the cone calorimeter, either 50 or 75 kW m^{-2} .

Finally, considering the obtained flame heat flux by the model and also a constant value for the flame heat flux taken from the literature [21], it is performed a redefinition of the linear fitting methodology, and the values for the HRR per unit area obtained with cone calorimeter under the heat fluxes of 75 and 25 kW m^{-2} are calculated. Errors of the

different methodologies are compared in order to choose the one that better allows cable cone calorimeter tests under different heat fluxes.

In order to compare the different methodologies results, the standard deviation ($\bar{\sigma}$) is calculated for the HRR per unit area curves. Additionally, it is included the calculation of the relative error for the prediction of the HRR per unit area peak value.

Results

In this section, the results of the global method application to find the best linear fitting are included. They are applied to five different cables ranging the class from Eca to B2ca, which gives information about the accuracy of the proposed linear fitting methodologies.

1st Stage

Cone calorimeter tests were performed as defined in the Materials and Method section. Then, Table 2 contains the ignition time (t_{ign}), the duration of the fire (Δt), calculated as difference between flameout and ignition time, the HRR per unit area peaks, the total heat release (THR), and the efficient heat of combustion average (EHC_{aver}) obtained from the experimental tests [20]. As we can see, time to ignition is influenced by the cable class for the analysed conditions of the cone calorimeter tests. As the results show, the lower time to ignition is found for the cables RV-k 0.6/1 kV $3 \times 1.5 \text{ mm}^2$ and RV-k 0.6/1 kV $3 \times 4 \text{ mm}^2$ with the class Eca. Similar time to ignition is found between the cables with the class Cca and B2ca. Nevertheless, in the cable with the class B2ca, the THR is the lowest, and the duration of

Table 2 Selected cables and properties

Cable	Heat flux	t_{ign}/s	$\Delta t/\text{s}$	$\text{HRR}_{\text{peak1}}/\text{kW m}^{-2}$	$\text{HRR}_{\text{peak2}}/\text{kW m}^{-2}$	THR/MJ m^{-2}	$\text{EHC}_{\text{aver}}/\text{kJ kg}^{-1}$
RV-k 0.6/1 kV $3 \times 1.5 \text{ mm}^2$	75 kW m^{-2}	8.0	992.0	224.8	329.5	135.6	20,425.5
	50 kW m^{-2}	24.0	1356.0	159.4	250.0	125.4	19,724.6
RV-k 0.6/1 kV $3 \times 4 \text{ mm}^2$	75 kW m^{-2}	10.5	1005.0	206.2	363.8	151.8	20,703.3
	50 kW m^{-2}	23.0	1270.0	139.5	273.9	149.1	22,040.5
RZ1-K AS $3 \times 1.5 \text{ mm}^2$	75 kW m^{-2}	44.0	1109.7	150.3	200.5	140.7	22,149.8
	50 kW m^{-2}	88.3	1732.0	100.1	171.1	154.5	22,540.4
	25 kW m^{-2}	392.0	2693.0	62.6	88.4	98.2	15,274.1
RZ1-K AS $5 \times 1.5 \text{ mm}^2$	75 kW m^{-2}	42.7	2007.0	150.3	175.9	180.6	20,026.4
	50 kW m^{-2}	93.0	2985.7	104.9	134.2	159.4	21,101.2
H07Z1-K $1 \times 50 \text{ mm}^2$	75 kW m^{-2}	44.3	899.0	185.0	302.0	99.1	20,278.0
	50 kW m^{-2}	110.7	1254.7	131.8	198.0	100.9	18,489.9
	25 kW m^{-2}	477.0	1956.3	62.9	92.4	87.1	17,861.9

the combustion is lower than the occurred for cables with the classification Cca. That means that although their ignition is similar, combustion is less intense in the cables B2ca than in the cables Cca, as expected. On Table 2, we can also see, that the total heat release is similar, even lower for the cables Eca, comparing to the cables Cca. Nevertheless, the cables Eca have a higher HRR per unit area peak and the duration of the combustion is lower, what is an indicative of the higher severity of the fire.

Figure 3 includes the compilation of the HRR per unit area curves for the different cone calorimeter tests. Black lines correspond to the heat flux of 75 kW m⁻², red lines to the heat flux of 50 kW m⁻² and blue lines to the heat flux of 25 kW m⁻². It can be clearly seemed that, as expected, the HRR per unit area values increase with the cone heat flux, while the time to peaks and duration of the tests decrease with the heat flux increase. This figure shows the effect of the cone heat flux in the samples. As higher is the cone calorimeter heat flux, as higher is the HRR per unit area peak value, and as early in time does it takes place.

2nd Stage

The following equations allows to directly apply the methodology defined in the FDS Guide [6] to rescale the time (Eq. 1) and the HRR per unit area (Eq. 2) values.

$$t_{HF_{New}} = t_{HF_0} \cdot \frac{CHF_0}{CHF_{New}} \tag{1}$$

$$HRR_{HF_{New}} = HRR_{HF_0} \cdot \frac{CHF_{New}}{CHF_0} \tag{2}$$

where CHF is the cone incident heat flux in kW m⁻², t_{HF} is the time in s, HRR_{HF} the heat release rate per unit area, the subscript “0” refers to the base experimental data and the subscript “New” refers to the desired value.

In the present work, the experimental cone calorimeter tests performed under the heat flux of 50 kW m⁻² have been employed as base tests to apply the methodology and predict cone calorimeter tests under the heat fluxes of 75 and

Fig. 3 Experimental cone calorimeter HRR curves under the heat fluxes of 25, 50 or/and 75 kW m⁻²: **a** RV-k 0.6/1 kV 3 × 1.5 mm²; **b** RV-k 0.6/1 kV 3 × 4 mm²; **c** RZ1-K AS 3 × 1.5 mm²; **d** RZ1-K AS 5 × 1.5 mm²; **e** H07Z1-K 1 × 50 mm²

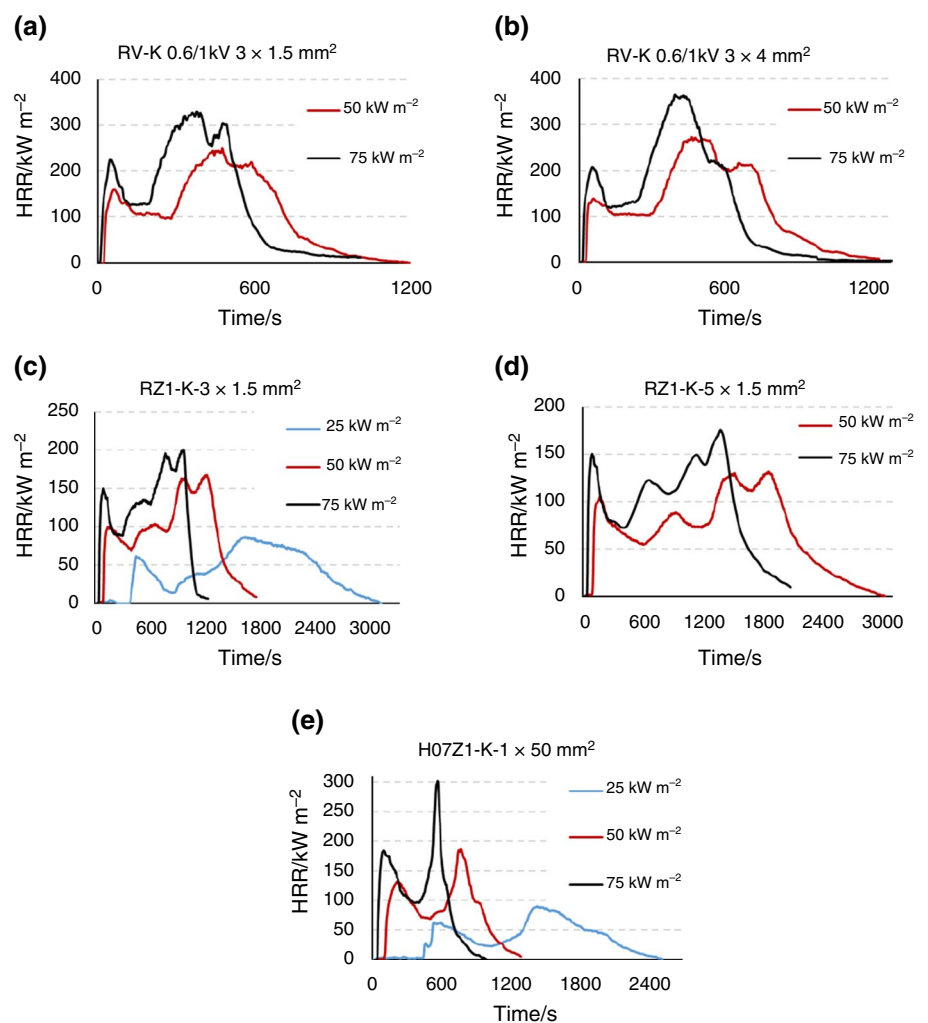
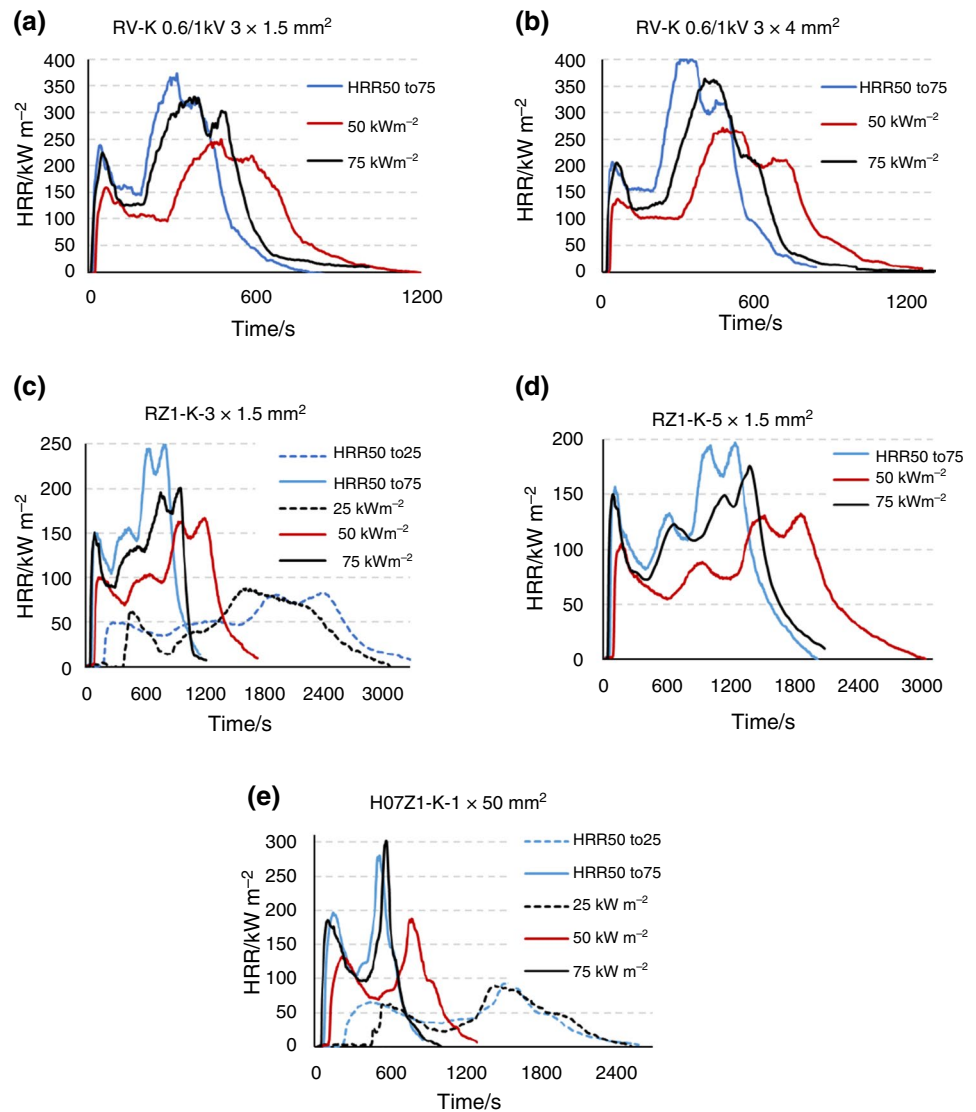


Fig. 4 Comparison of the calculated and experimental cone calorimeter HRR per unit area curves under the heat fluxes of 25 or/and 75 kW m⁻²: **a** RV-k 0.6/1 kV 3 × 1.5 mm²; **b** RV-k 0.6/1 kV 3 × 4 mm²; **c** RZ1-K AS 3 × 1.5 mm²; **d** RZ1-K AS 5 × 1.5 mm²; **e** H07Z1-K 1 × 50 mm²



25 kW m⁻². This methodology has been applied directly by the analytical Eqs. (1) and (2), that are the ones applied internally by FDS. Results of the application of this methodology are shown on Fig. 4 for the different cables. Red line defines the experimental cone calorimeter result under the heat flux of 50 kW m⁻², black solid lines represent the experimental cone calorimeter results under the heat flux of 75 kW m⁻², and blue solid lines are used for the HRR per unit area predicted by the FDS Guide methodology for the heat flux of 75 kW m⁻². Black and blue dashed lines represent the experimental and predicted curves for the heat flux of 25 kW m⁻², respectively.

The standard deviation of the HRR per unit area predictions performed with the application of the FDS Guide methodology are compiled on Table 3. It can be seen

Table 3 Standard deviation of the HRR per unit area predictions with the FDS Guide methodology

Cable	HF 75 kW m ⁻²	HF 25 kW m ⁻²
	$\tilde{\sigma}_{50\text{ to }75}/\text{kW m}^{-2}$	$\tilde{\sigma}_{50\text{ to }25}/\text{kW m}^{-2}$
RV-k 0.6/1 kV 3 × 1.5 mm ²	55.6	–
RV-k 0.6/1 kV 3 × 4 mm ²	73.8	–
RZ1-K AS 3 × 1.5 mm ²	50.3	20.9
RZ1-K AS 5 × 1.5 mm ²	32.4	–
H07Z1-K 1 × 50 mm ²	41.6	18.3

that the highest deviations are found in the cables RV-k 0.6/1 kV 3 × 1.5 mm² and RV-k 0.6/1 kV 3 × 4 mm² with

Table 4 Values and relative error of the HRR per unit area peak predictions with the FDS guide methodology

Cable	CC75 Exp. HRR peak/ kW m ⁻²	CC75. 50to75 HRR peak/kW m ⁻²	CC75. 50to75 HRR peak error/%
RV-k 0.6/1 kV 3 × 1.5 mm ²	329.47	374.94	13.80
RV-k 0.6/1 kV 3 × 4 mm ²	363.77	403.49	10.92
RZ1-K AS 3 × 1.5 mm ²	200.47	251.26	25.33
RZ1-K AS 5 × 1.5 mm ²	175.87	197.87	12.51
H07Z1-K 1 × 50 mm ²	301.96	279.95	- 7.29

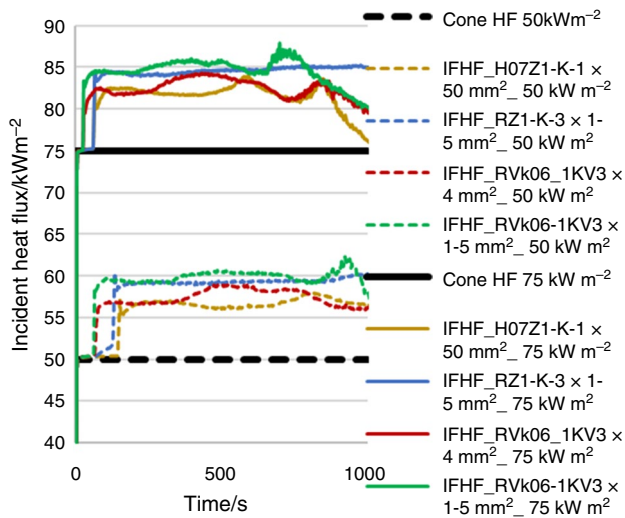


Fig. 5 Incident heat flux in the sample surface for simulated cone calorimeter under heat flux of 50 kW m⁻² and 75 kW m⁻²

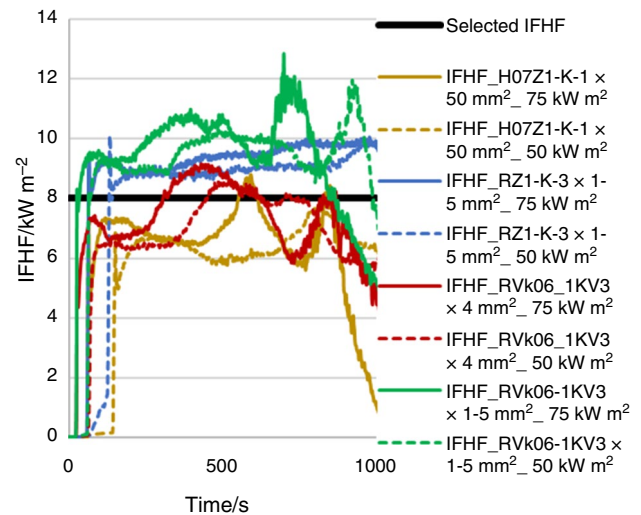


Fig. 6 Calibration of the incident heat flux in the sample Surface for cone calorimeter heat flux of 50 kW m⁻² and 75 kW m⁻²

the class Eca. It can be also seen that the standard deviation is lower in the prediction of the cone calorimeter tests under a heat flux of 25 kW m⁻². On Table 4, the experimental and predicted values for the HRR per unit area peak are presented, and the relative error of the prediction. The highest error is found for the cable RZ1-K AS 3 × 1.5 mm² (classification Cca), and has a value of around 25%. All cases overestimate the peak values except for the cable H07Z1-K 1 × 50 mm² (classification B2ca) that underestimates it.

3rd Stage

In the third stage, the influence of the flame in the decomposition of the sample in the cone calorimeter is evaluated. In the previous stage, following the methodology defined in the FDS Guide, the incident heat flux considered was the imposed by the cone calorimeter. Nevertheless, the reradiation effect of the flames generated during combustion is not considered. To evaluate this reradiation, also called flame

heat flux (FHF), we include two approaches in the present work: (1) estimating this value by a computational model of the cone calorimeter tests; (2) considering experimental results taken from the literature.

Firstly, the model of the cone calorimeter tests was performed with the model FDS. Calibrations of the incident heat fluxes were performed by considering an inert sample. When cone calorimeter FDS model is calibrated to impose desired heat flux in the sample, the HRR per unit area curve obtained experimentally in each cable test is imposed as input in the modelled sample material. A device to measure the total incident heat flux in the sample surface is included in the centre of the sample. This total incident heat flux will include the cone calorimeter heat flux (50 kW m⁻² or 75 kW m⁻² in our case) and the flame heat flux (heat feedback). Figure 5 shows the cone calorimeter heat fluxes (50 kW m⁻² and 75 kW m⁻²) and the total incident heat fluxes measured in the simulation. The flame heat flux is calculated as the difference between the total incident heat flux measured in

the simulations (coloured lines in Fig. 5) and the cone calorimeter heat flux defined to perform the tests (black lines in Fig. 5). Finally, the FHF for the different cables can be observed on Fig. 6. A constant value of FHF for all cables has been defined, taking as average a value of 8 kW m^{-2} . A constant FHF value is also suggested to allow its use in computational models like FDS.

Secondly, the experimental value considered for the FHF has been taken from [21]. In this work the procedure followed is based on the obtention of a constant flame heat flux. This constant value occurs for flames above the top of the cone heater. A constant net flame heat flux of approximately 20 kW m^{-2} for nylon 6/6, 19 kW m^{-2} for polyethylene, 11 kW m^{-2} for polypropylene and 28 kW m^{-2} for black PMMA is obtained for irradiation levels ranging from 0 to 90 kW m^{-2} . As all the cables employed in the present work with a class of Cca or Eca have cross-linked polyethylene in their insulation, we have selected an FHF of 19 kW m^{-2} .

4th Stage

Finally, we present a method to take into account the effect of the FHF in the linear fitting methodology defined in FDS Guide (previous Eqs. 1 and 2). Proposed linear fitting methodology is similar when considering the simulated FHF, FHF_{FDS} , (Eqs. 3 and 4) and the experimental FHR, FHF_{Lit} , (Eqs. 5 and 6) with the only difference in the value of the FHF.

$$t_{\text{HF}_{\text{New}}} = t_{\text{HF}_0} \cdot \frac{\text{CHF}_0 + \text{FHF}_{\text{FDS}}}{\text{CHF}_{\text{New}} + \text{FHF}_{\text{FDS}}} \quad (3)$$

$$\text{HRR}_{\text{HF}_{\text{New}}} = \text{HRR}_{\text{HF}_0} \cdot \frac{\text{CHF}_{\text{New}} + \text{FHF}_{\text{FDS}}}{\text{CHF}_0 + \text{FHF}_{\text{FDS}}} \quad (4)$$

$$t_{\text{HF}_{\text{New}}} = t_{\text{HF}_0} \cdot \frac{\text{CHF}_0 + \text{FHF}_{\text{Lit}}}{\text{CHF}_{\text{New}} + \text{FHF}_{\text{Lit}}} \quad (5)$$

$$\text{HRR}_{\text{HF}_{\text{New}}} = \text{HRR}_{\text{HF}_0} \cdot \frac{\text{CHF}_{\text{New}} + \text{FHF}_{\text{Lit}}}{\text{CHF}_0 + \text{FHF}_{\text{Lit}}} \quad (6)$$

Table 5 Values of the CHF+FHF for the FHF obtained from FDS simulation and from literature

FHF source	FHF value/ kW m^{-2}	CHF + FHF		
		CHF = 75 kW m^{-2}	CHF = 50 kW m^{-2}	CHF = 25 kW m^{-2}
From FDS simulation	8	83	58	33
From literature [21]	19	94	69	44

The calculated sums of CHF + FHF for the different cases are included in Table 5. These values are the total incident heat fluxes that affect the decomposition of the sample.

On Fig. 7 are compared the curves obtained as results of the application of the methodologies used to estimate the HRR per unit area under the heat fluxes of 75 and 25 kW m^{-2} . The solid lines are used for the heat flux of 75 kW m^{-2} and the dashed lines for the 25 kW m^{-2} cone calorimeter tests. The black lines represent the experimental results; the blue lines indicate the approximation using the FDS guide methodology (legend HRR50to75 that means a CHF_0 of 50 kW m^{-2} and a CHF_{New} of 75 kW m^{-2}); the red lines define the results obtained by using the FHF_{FDS} (legend HRR58to83 that means a $\text{CHF}_0 + \text{FHF}_{\text{FDS}}$ of 58 kW m^{-2} and a $\text{CHF}_{\text{New}} + \text{FHF}_{\text{FDS}}$ of 83 kW m^{-2}), and finally, the purple lines represent the results for the methodology that employs the FHF_{Lit} (legend HRR69to94 that means a $\text{CHF}_0 + \text{FHF}_{\text{Lit}}$ of 69 kW m^{-2} and a $\text{CHF}_{\text{New}} + \text{FHF}_{\text{Lit}}$ of 94 kW m^{-2}). As we can observe, the time to ignition is properly predicted when the heat flux has a value of 75 kW m^{-2} , with the exception of the cable H07Z1-K $1 \times 50 \text{ mm}^2$ (B2ca class). The ignition time is also not predicted for the two cables tested under 25 kW m^{-2} heat flux. The methodology that considers FHF value from literature makes a better prediction of the experimental HRR per unit area curve when the heat flux is 75 kW m^{-2} for the cables with classifications Eca and Cca.

The standard deviation of the HRR per unit area predictions made by the methodologies are included on Table 6. It can be noticed how the standard deviations decrease in those methodologies that consider the FHF when the heat flux is 75 kW m^{-2} , especially when the FHF used is the one taken from the literature. With this value, standard deviation decreases about to the half of the standard deviation obtained with the methodology defined in the FDS Guide for the cables with the class Eca and Cca. Nevertheless, when heat flux is 25 kW m^{-2} , the standard deviation increases with the methodologies that consider the FHF.

Tables 7 and 8 include the experimental and predicted values for the HRR per unit area peak obtained in the cone calorimeter tests with a heat flux of 75 kW m^{-2} , and the relative error of the predictions, respectively. The HRR per unit area peak value prediction improves by considering the FHF taken from the literature for the four cables with the classes Eca and Cca, decreasing the error from 13.8% to 3.4% for the cable RV-k $0.6/1 \text{ kV } 3 \times 1.5 \text{ mm}^2$, from 10.9 to 2.2% for the cable RV-k $0.6/1 \text{ kV } 3 \times 4 \text{ mm}^2$, from 25.3 to 13.8% for the cable RZ1-K AS $3 \times 1.5 \text{ mm}^2$ and from 12.5 to 2.2% for the cable RZ1-K AS $5 \times 1.5 \text{ mm}^2$. Nevertheless, it increases for the cable H07Z1-K $1 \times 50 \text{ mm}^2$, with the classification B2ca, increasing from an error of -7.3% with the FDS methodology to 15.6% with the consideration of the FHF taken from the literature.

Fig. 7 Comparison of the calculated and experimental cone calorimeter HRR per unit area curves: **a** RV-k 0.6/1 kV $3 \times 1.5 \text{ mm}^2$ (HF 75 kW m^{-2}); **b** RV-k 0.6/1 kV $3 \times 4 \text{ mm}^2$ (HF 75 kW m^{-2}); **c** RZ1-K AS $3 \times 1.5 \text{ mm}^2$ (HF 75 kW m^{-2}); **d** RZ1-K AS $3 \times 1.5 \text{ mm}^2$ (HF 25 kW m^{-2}); **e** RZ1-K AS $5 \times 1.5 \text{ mm}^2$ (HF 75 kW m^{-2}); **f** H07Z1-K $1 \times 50 \text{ mm}^2$ (HF 75 kW m^{-2}); **g** H07Z1-K $1 \times 50 \text{ mm}^2$ (HF 25 kW m^{-2})

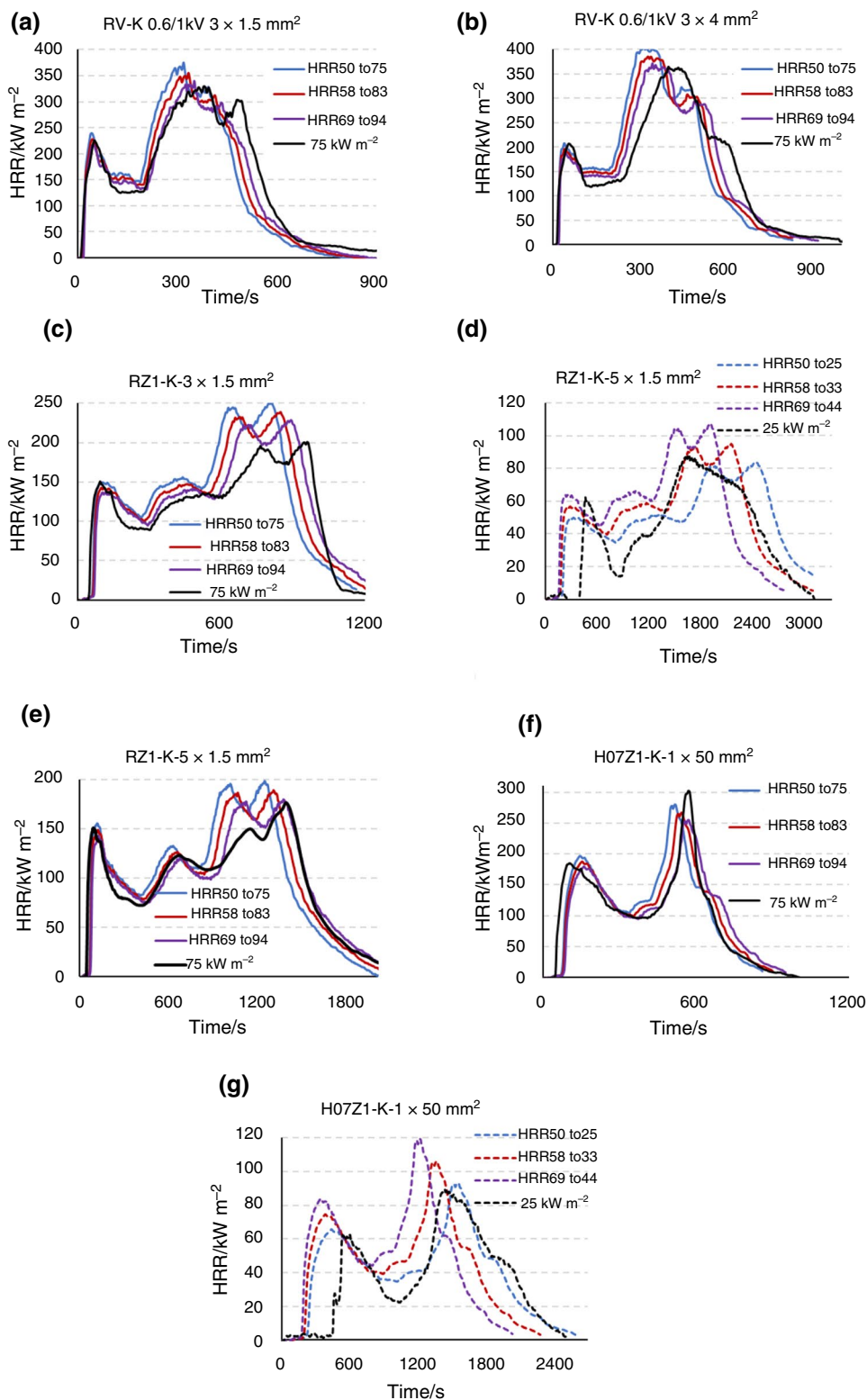


Table 6 Standard deviation of the HRR per unit area predictions with the different methodologies

Cable	HF 75 kW m ⁻²			HF 25 kW m ⁻²		
	$\bar{\sigma}_{50\text{ to }75}/\text{kW m}^{-2}$	$\bar{\sigma}_{58\text{ to }83}/\text{kW m}^{-2}$	$\bar{\sigma}_{69\text{ to }94}/\text{kW m}^{-2}$	$\bar{\sigma}_{50\text{ to }25}/\text{kW m}^{-2}$	$\bar{\sigma}_{58\text{ to }33}/\text{kW m}^{-2}$	$\bar{\sigma}_{69\text{ to }44}/\text{kW m}^{-2}$
RV-k 0.6/1 kV 3×1.5 mm ²	55.6	40.7	27.1	–	–	–
RV-k 0.6/1 kV 3×4 mm ²	73.8	58.5	44.5	–	–	–
RZ1-K AS 3×1.5 mm ²	50.3	39.5	28.5	20.9	19.6	29.9
RZ1-K AS 5×1.5 mm ²	32.4	22.8	16.8	–	–	–
H07Z1-K 1×50 mm ²	41.6	32.0	32.8	18.3	28.1	43.7

Table 7 Values of the HRR per unit area peak predictions with the different methodologies

Cable	CC75 Exp. HRR peak/kW m ⁻²	CC75. 50to75 HRR peak/kW m ⁻²	CC75. 58to83 HRR peak/kW m ⁻²	CC75. 69to94 HRR peak/kW m ⁻²
RV-k 0.6/1 kV 3×1.5 mm ²	329.5	375.0	356.1	340.5
RV-k 0.6/1 kV 3×4 mm ²	363.8	403.5	385.5	371.9
RZ1-K AS 3×1.5 mm ²	200.5	251.3	239.4	228.2
RZ1-K AS 5×1.5 mm ²	175.9	197.9	188.7	179.7
H07Z1-K 1×50 mm ²	302.0	280.0	267.1	255.0

Table 8 Relative error of the HRR per unit area peak predictions with the different methodologies

Cable	CC75. 50to75 HRR peak error/%	CC75. 58to83 HRR peak error/%	CC75. 69to94 HRR peak error/%
RV-k 0.6/1 kV 3×1.5 mm ²	13.8	8.1	3.4
RV-k 0.6/1 kV 3×4 mm ²	10.9	6.0	2.2
RZ1-K AS 3×1.5 mm ²	25.3	19.4	13.8
RZ1-K AS 5×1.5 mm ²	12.5	7.3	2.2
H07Z1-K 1×50 mm ²	– 7.3	– 11.6	– 15.6

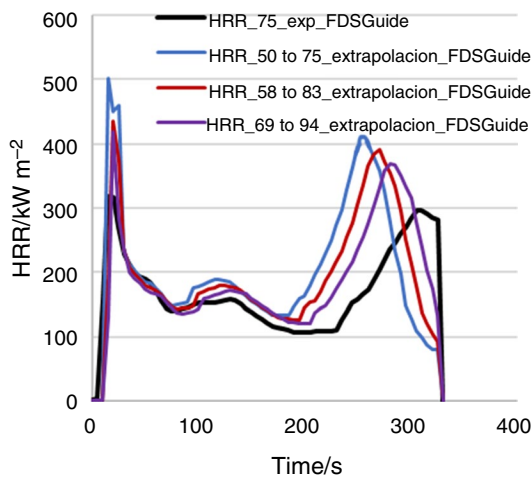


Fig. 8 Comparison of the calculated and experimental cone calorimeter HRR per unit area curves for the FDS Guide example under the heat flux of 75 kW m⁻²

Table 9 Standard deviation of the HRR per unit area predictions with the different methodologies

Sample	HF 75 kW m ⁻²		
	$\bar{\sigma}_{50\text{ to }75}/\text{kW m}^{-2}$	$\bar{\sigma}_{58\text{ to }83}/\text{kW m}^{-2}$	$\bar{\sigma}_{69\text{ to }94}/\text{kW m}^{-2}$
Example FDS guide [6]	111.4	87.6	63.7

Table 10 Values of the HRR per unit area peak and relative error of the HRR per unit area peak predictions with the different methodologies

Cable	HRR peak1/kW m ⁻²	HRR peak2/kW m ⁻²	HRR peak1 error/%	HRR peak2 error/%
Experimental	343.8	299.6	–	–
HRR 50to75 kW m ⁻²	479.0	410.9	39.3	37.1
HRR 58to83 kW m ⁻²	457.0	392.0	32.9	30.8
HRR 69to94 kW m ⁻²	435.1	373.2	26.5	24.5

Discussions

Finally, we present the comparison of the results of the application of the methodologies to the cone calorimeter test example included in the FDS Guide [6] first, and then to the cone calorimeter tests on 7 typical cables of nuclear power plants from the NUREG 7010 [4] and from [22].

Firstly, Fig. 8 shows the comparison of the HRR per unit area experimental curve (black line) with the obtained with the methodology defined in the FDS Guide (blue line), the methodology that considers the FHF_{FDS} (red line) and the methodology that employs the $IFHF_{Lit}$ (purple line). Whereas the time at which the first peak takes place is correctly predicted in all cases, the time of the second peak is better predicted with the methodology that considers FHF_{Lit} . As we can see, all cases produce higher values of the HRR per unit area curve than the original curve. This makes these methodologies to be in the side of the safety.

Table 9 includes the standard deviation of the HRR per unit area predictions. As occurred with the cone calorimeter experimental tests included in the Results section, the prediction improves with the consideration of the FHF_{Lit} . In this example, the standard deviation decreases from 110.6 kW m^{-2} with the FDS Guide methodology to 63.2 kW m^{-2} with the methodology that considers the FHF_{Lit} . Table 10 includes the comparison of the HRR per unit area peak values and the error of the estimated with the different methodologies. It can be noticed an important descent in the error when of the FHF_{Lit} is considered.

Now, the application of the different analysed methodologies to several cables taken from the literature is included. The description of the 6 cables selected from the NUREG 7010 [4] is shown in Table 11. In these cables, the cone calorimeter HRR obtained with a heat flux of 50 kW m^{-2} will be considered as input to estimate the cone calorimeter HRR results under a heat flux of 75 kW m^{-2} with the different methodologies.

Finally, a halogen-free flame-retardant cable with a diameter of 12 mm taken from [22] is analysed. In this case the cone calorimeter heat flux considered as input is 47 kW m^{-2} and the target is the heat flux of 70 kW m^{-2} . Table 12 contains the calculation of the CHF + FHF for the methodology defined in FDS Guide [6] and for the defined in the present paper considering the FDS simulation and the literature [21].

Figure 9 compares the curves obtained as results of the application of the methodologies used to estimate the HRR per unit area under the heat flux of 75 for the different cables taken from literature. The black lines represent the experimental results; the blue lines indicate the approximation using the FDS guide methodology; the red lines define the results obtained by using the FHF estimated from FDS simulation, and finally, the purple lines represent the results for the methodology that employs the FHF taken from literature. As we can observe, the time to ignition and time of the first peak is properly predicted in all cables by all methodologies. However, more discrepancies are found in the second peak, where prediction by the methodology that employs the FHF taken from literature achieves a better approximation. Nevertheless, as Fig. 9 shows, all methodologies can reproduce

Table 11 Selected NUREG 7010 cables and properties

Cable	Diameter/mm	Sheath material	Insulation material
NU11	32.0	Chloro-sulfanated polyethylene CSPE	Cross-linked polyethylene XLPE
NU16	19.0	Neoprene	Cross-linked polyethylene XLPE
NU23	14.0	Chloro-sulfanated polyethylene CSPE	Cross-linked polyethylene XLPE
NU219	14.0	Chloro-sulfanated polyethylene CSPE	Ethylene-propylene rubber EPR
NU367	16.0	–	Ethylene-propylene rubber EPR
NU701	14.0	Polyvinyl chloride PVC	Polyethylene PE

Table 12 Values of the CHF + FHF for the FHF obtained from FDS simulation and from the literature

FHF source	FHF value/ kW m^{-2}	CHF + FHF			
		CHF = 50 kW m^{-2}	CHF = 47 kW m^{-2}	CHF = 75 kW m^{-2}	CHF = 70 kW m^{-2}
From FDS guide [6]	0	50	47	75	70
From FDS simulation	8	58	55	83	78
From literature [21]	19	69	66	94	89

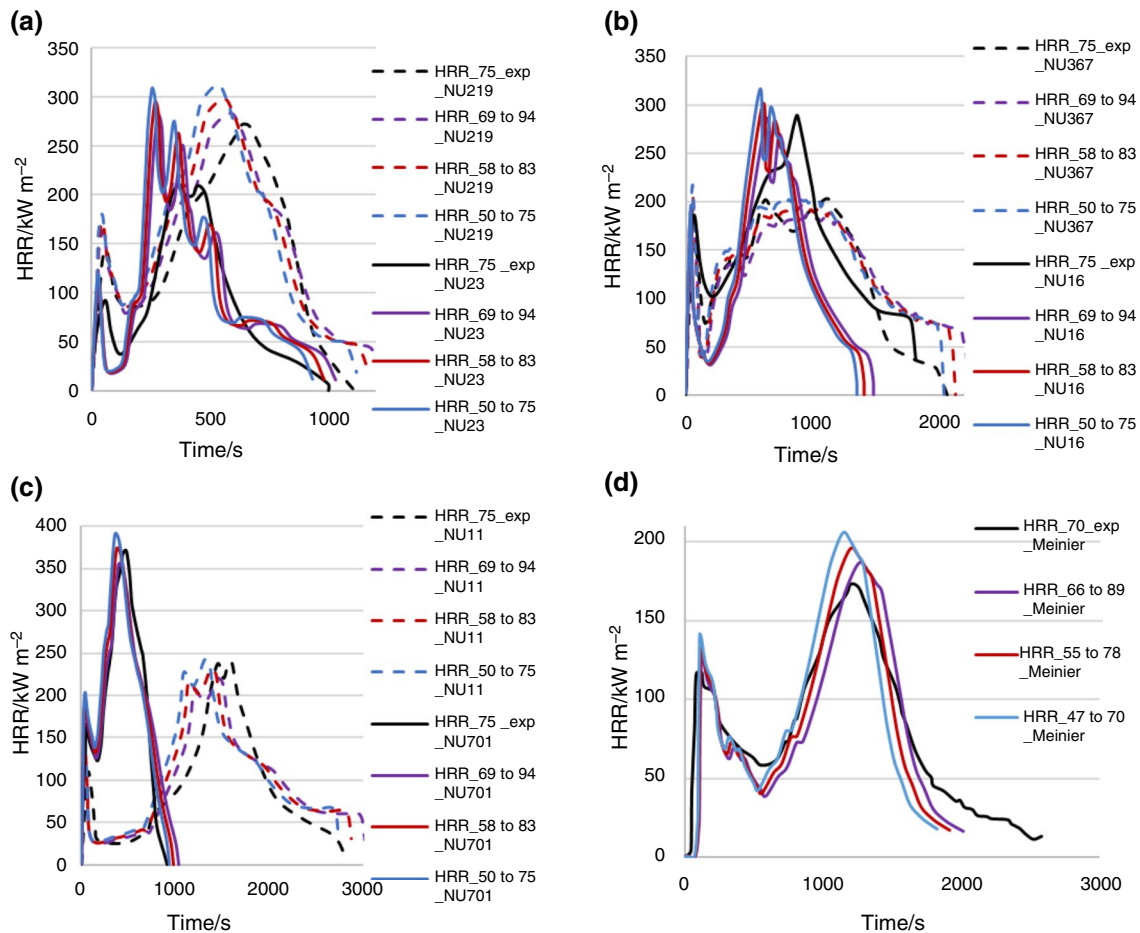


Fig. 9 Comparison of the calculated and experimental cone calorimeter HRR per unit area curves: **a** NU219 and NU23 (HF 75 kW m⁻²); **b** NU367 and NU16 (HF 75 kW m⁻²); **c** NU11 and NU701 (HF 75 kW m⁻²); **d** Meinier cable (HF 70 kW m⁻²)

the behavior of the cables under the highest heat fluxes (75 and 70 kW m⁻²).

Table 13 includes the standard deviation of the HRR per unit area predictions made by the methodologies for

Table 13 Standard deviation of the HRR per unit area predictions with the different methodologies

Cable	$\tilde{\sigma}_{\text{From FDS Guide/}} / \text{kW m}^{-2}$	$\tilde{\sigma}_{\text{From FDS Simulation/}} / \text{kW m}^{-2}$	$\tilde{\sigma}_{\text{From Literature/}} / \text{kW m}^{-2}$
NU11 [4]	44.8	36.5	28.9
NU16 [4]	76.3	68.9	62.3
NU23 [4]	53.8	47.3	41.3
NU219 [4]	49.8	37.2	26.6
NU367 [4]	27.8	28.0	29.3
NU701 [4]	47.1	40.3	40.4
Meinier et al. [22]	27.7	23.1	23.2

The significant of italic values highlight the lower standard deviations for every cable

the different cables. It can be noticed how the standard deviations decrease in those methodologies that consider the FHF taken from FDS simulation ($\tilde{\sigma}_{\text{From FDS Simulation}}$) and from literature ($\tilde{\sigma}_{\text{From Literature}}$) except for the cable NU367, where deviation is slightly lower in the estimation performed by the FDS guide methodology ($\tilde{\sigma}_{\text{From FDS Guide}}$). The deviation in NU701 and Meinier cables are very similar in the estimation considering the FDS simulation and the literature value of the FHF, while for the other cables is lower when the FHF used is the one from the literature. This may be related with the polyethylene contained in the cables, since the FHF considered correspond to PE and these cables are made without it. Finally, Table 14 includes the comparison of the HRR per unit area peak values and the error of the estimated with the different methodologies. It can be noticed in the mean relative error an important descent in the error when of the FHF is considered, both taken from simulation or from literature.

Table 14 Values of the HRR per unit area peak and relative error of the HRR per unit area peak predictions with the different methodologies for the literature cables

Cable	HRR _{peak} Exp/ kW m ⁻²	HRR _{peak} FDS- Guide/kW m ⁻²	HRR _{peak} FDS- Sim./kW m ⁻²	HRR _{peak} FDSLit./ kW m ⁻²	HRR _{peak} FDS- Guide error/%	HRR _{peak} FDS- Sim. error/%	HRR _{peak} FDSLit error/%
NU11 [4]	238.1	241.7	230.5	219.5	1.5	- 3.2	- 7.8
NU16 [4]	288.3	315.8	298.8	285.8	9.5	3.6	- 0.9
NU23 [4]	209.2	308.4	291.9	280.7	47.4	39.5	34.2
NU219 [4]	271.4	312.2	297.7	283.8	15.0	9.7	4.6
NU367 [4]	202.3	207.2	197.7	188.1	2.4	- 2.3	- 7.0
NU701 [4]	372.2	391.2	373.6	355.6	5.1	0.4	- 4.5
Meinier [22]	173.5	205.8	196.1	186.3	18.6	13.0	7.4
Mean relative error					14.2	10.2	9.5

Conclusions

This work aims at analysing and predicting the effect of the cone calorimeter heat flux in the heat release rate per unit area of samples composed by cables. To do so, it has been evaluated a linear fitting methodology defined in the FDS Guide to extrapolate the HRR per unit area between different heat fluxes. Additionally, a variation in the methodology has been proposed. This variation intends to consider the effect of the flame heat flux in the decomposition of the sample, hence, on the HRR per unit area. To validate the proposed methodologies, an experimental campaign has been defined, testing 5 different cable types under several heat fluxes. These tests have been carried out using the cone calorimeter. Finally, it has been also applied to seven additional cables taken from literature.

In order to apply the proposed methodologies, the flame heat flux has been calculated with a model of the cone calorimeter test performed in FDS. A flame heat flux value of 8 kW m⁻² was obtained with the computational analysis for the analysed cables, since an experimental value of 19 kW m⁻² was obtained from the literature for the polyethylene [21]. The linear fittings considering the flame heat flux influence with the computational and experimental values are presented, showing some improvements in the results from considering the cone calorimeter incident heat flux only. Results show that the linear fitting with the consideration of the experimental flame heat flux taken from literature leads in general to improvements in the prediction of the HRR per unit area. As the flame heat flux was taken from the polyethylene, the results for cable H07Z1-K 1 × 50 mm², which does not have polyethylene, get worse comparing to the methodology that considers the flame heat flux computationally estimated. Proposed methodologies address better the estimation of the HRR for high incident heat fluxes, this can be related with the fact that the lower cone calorimeter flux (25 kW m⁻²) are close to the critical heat flux and decomposition behavior of cables vary. Application of the

methodologies to the cone calorimeter tests on cables analyzed in the FDS Validation Guide [7], and included in the NUREG 7010 [4] and in [22] shows an improvement in the accuracy of the representation of the HRR release for higher incident heat fluxes with the methodologies that consider the FHF, obtained from simulation and from literature.

Methodology using PE FHF literature value seems to be the most suitable for the cables that contain PE. More studies are needed to experimentally analyse incident heat flux in the cone calorimeter tests and use it in the proposed methodology.

Acknowledgements This work has been previously presented in the 1st Central and Eastern European Conference on Physical Chemistry & Materials Science (CEEC-PCMS1). The authors are grateful to the organization for their collaboration. The authors would like to thank the Consejo de Seguridad Nuclear for the cooperation and co-financing of the project "Metodologías avanzadas de análisis y simulación de escenarios de incendios en centrales nucleares".

Funding Open Access funding provided thanks to the CRUE-CSIC agreement with Springer Nature.

Open Access This article is licensed under a Creative Commons Attribution 4.0 International License, which permits use, sharing, adaptation, distribution and reproduction in any medium or format, as long as you give appropriate credit to the original author(s) and the source, provide a link to the Creative Commons licence, and indicate if changes were made. The images or other third party material in this article are included in the article's Creative Commons licence, unless indicated otherwise in a credit line to the material. If material is not included in the article's Creative Commons licence and your intended use is not permitted by statutory regulation or exceeds the permitted use, you will need to obtain permission directly from the copyright holder. To view a copy of this licence, visit <http://creativecommons.org/licenses/by/4.0/>.

References

1. Chen R, Lu S, Li C, Ding Y, Zhang B, Lo S. Correlation analysis of heat flux and cone calorimeter test data of commercial flame-retardant ethylene-propylene-diene monomer (EPDM) rubber. J

- Therm Anal Calorim. 2016;123:545–56. <https://doi.org/10.1007/s10973-015-4900-x>.
2. McGrattan K, Hostikka S, Floyd J, McDermott R, Vanella M. NIST special publication 1019 sixth edition fire dynamics simulator user's guide. NIST, VTT, 2021.
 3. U.S.NRC The Browns Ferry Nuclear Plant Fire of 1975 and the history of NRC fire regulations, 2009.
 4. NUREG/CR-6738, SAND2001-1676P, risk methods insights gained from fire incidents. Sandia National Laboratories, U.S. NRC, 2001.
 5. NUREG-1925, Rev. 4, research activities FY 2018–2020. U. S. NRC, Washington, D.C., March 2018.
 6. NUREG/CR-7010 cable heat release, ignition, and spread in tray installations during fire (CHRISTIFIRE), phase 1: horizontal trays. 2012.
 7. NUREG/CR-7010 cable heat release, ignition, and spread in tray installations during fire (CHRISTIFIRE), phase 2: vertical shafts and corridors. 2013.
 8. McGrattan K, Hostikka S, Floyd J, McDermott R, Vanella M. NIST special publication 1018–3 sixth edition fire dynamics simulator technical reference guide volume 3: validation. VTT, NIST, 2022.
 9. Bascou S, Suard S, Audouin L. Benchmark activity of the OECD/NEA PRISME 3 and FIRE projects. In: 25th international conference on structural mechanics in reactor technology (SMiRT 25), 16th international post-conference seminar on “fire safety in nuclear power plants and installations”, SMiRT, Ottawa, Canada, 2019.
 10. Spille J, Riese O, Zehfu J. Experimental and numerical investigations of the influence of cable arrangements on cable trays concerning mass loss rate and fire propagation. SMiRT 24. In: 15th international seminar on fire safety in nuclear power plants and installations, Bruges, Belgium, 2017.
 11. Liang K, Hao X, An W, Tang Y, Cong Y. Study on cable fire spread and smoke temperature distribution in T-shaped utility tunnel. Case Stud Therm Eng. 2019. <https://doi.org/10.1016/j.csite.2019.100433>.
 12. Siemon M, Riese O, Forell B, Krönung D, Klein-Heßling W. Experimental and numerical analysis of the influence of cable tray arrangements on the resulting mass loss rate and fire spreading. Fire Mater. 2019;43(5):497–513. <https://doi.org/10.1002/fam.2689>.
 13. NEA/CSNI/R(2017)14, investigating heat and smoke propagation mechanisms in multi-compartment fire scenarios, final report of the PRISME project. OECD, NEA, January 2018.
 14. Beji T, Merci B. Numerical simulations of a full-scale cable tray fire using small-scale test data. Fire Mater. 2018. <https://doi.org/10.1002/fam.2687>.
 15. Grayson S, Van Hees P, Vercellotti U. Fire performance of electric cables: new test methods and measurement techniques. England: Interscience Communications Ltd; 2000.
 16. BS EN 60332-1-2 2004. Tests on electric and optical fibre cables under fire conditions—part 1–2: test for vertical flame propagation for a single insulated wire or cable—procedure for 1 kW pre-mixed flame.
 17. UNE-EN 50399:2012/A1:2016. Common test methods for cables under fire conditions—heat release and smoke production measurement on cables during flame spread test—test apparatus, procedures, results.
 18. Lázaro D, Lázaro M, Alonso A, Lázaro P, Alvear D. Influence of the STA boundary conditions on thermal decomposition of thermoplastic polymers. J Therm Anal Calorim. 2019;138:2457–68. <https://doi.org/10.1007/s10973-019-08787-4>.
 19. Alonso A, Lázaro D, Lázaro D, Alvear D. Self heating evaluation on thermal analysis of polymethyl methacrylate (PMMA) and linear low density polyethylene (LLDPE). J Therm Anal Calorim. 2022;147:10067–81. <https://doi.org/10.1007/s10973-022-11364-x>.
 20. ISO 5660-1:2015. reaction-to-fire tests—heat release, smoke production and mass loss rate—part 1: heat release rate (cone calorimeter method) and smoke production rate (dynamic measurement).
 21. Hopkins D Jr, Quintiere JG. Material fire properties and predictions for thermoplastics. Fire Saf J. 1996;26:241–68. [https://doi.org/10.1016/S0379-7112\(96\)00033-1](https://doi.org/10.1016/S0379-7112(96)00033-1).
 22. Meinier R, Sonnier R, Zavaleta P, Suard S, Ferry L. Fire behavior of halogen-free flame retardant electrical cables with the cone calorimeter. J Hazard Mater. 2018;342:306–16. <https://doi.org/10.1016/j.jhazmat.2017.08.027>.

Publisher's Note Springer Nature remains neutral with regard to jurisdictional claims in published maps and institutional affiliations.